NATURAL SCIENCE REVIEW 2 100304 (2025)
nsr.jinr.int

3D segmented neutrino detector SuperFGD

Yu. Kudenko*[1,2,3]

[1] *Institute for Nuclear Research, Russian Academy of Sciences, Moscow, Russia*
[2] *Moscow Institute of Physics and Technology, Moscow Region, Russia*
[3] *Moscow Engineering Physics Institute, Moscow, Russia*

Abstract

The near neutrino detector ND280 of the long-baseline accelerator experiment T2K has been upgraded to improve the precision of measurement of the neutrino oscillation parameters. A key component of the upgrade is a novel segmented plastic scintillator detector, Super Fine Grained Detector (SuperFGD), made of approximately 2 million optically isolated 1 cm^3 cubes read out by three orthogonal wavelength-shifting fibres and multi-pixel photon counters. The SuperFGD provides 3D images of neutrino interactions by tracking the final-state charged particles including protons down to a threshold of about 300 MeV/c. Due to the fine segmentation and the sub-nanosecond time resolution, the SuperFGD is able to detect neutrons from neutrino interactions and to reconstruct their kinetic energy by measuring the time of flight. In this paper, the details of the detector design, construction and performance in the T2K neutrino beam are described.

Keywords: neutrino oscillations, CP violation, neutrino detectors, scintillating segmented detector, wavelength-shifting fibres, multi-pixel photon counters

DOI: 10.54546/NaturalSciRev.100304

1. Introduction

The long-baseline accelerator experiment Tokai-to-Kamioka (T2K) [1] studies neutrino oscillations using a neutrino beam sent from the Japan Proton Accelerator Research Complex (J-PARC) in Tokai towards the 50 kt water Cherenkov detector Super-Kamiokande, located 295 km away in Kamioka. A near detector ND280 [2], situated 280 m downstream of the hadron production target at J-PARC, measures parameters of unoscillated neutrino spectra, constrains systematic uncertainties related to the neutrino flux and interaction cross section and detector acceptance. The ND280 has a good detection and reconstruction efficiency of charged particles from neutrino interactions in the forward region, but the efficiency drops considerably for angles larger than ~ 50 degrees with respect to the beam direction. On the other hand, Super-Kamiokande detects charged particles in the 4π solid angle with high efficiency. In addition, ND280 has a relatively high momentum threshold for protons. It should

*Corresponding author e-mail address: kudenko@inr.ru

Received: 12 May 2025; Revised: 3 June 2025; Accepted: 4 June 2025; Published: 20 June 2025

be noted that the reconstruction of low-momentum pions and protons is very important in order to study nuclear effects in neutrino interactions. ND280 is also not able to reconstruct the kinetic energy of neutrons produced in interactions of antineutrinos. The sensitivity of the T2K and Hyper-Kamiokande [3] experiments to CP violation requires reducing the systematic errors, which can be achieved by accurate measurements of the neutrino interaction cross sections. As statistics were collected, it became obvious that the ND280 needed to be upgraded to detect muons and pions in the full polar angle with good particle identification and momentum resolution, to measure and reconstruct low-energy protons with proton–pion separation, and to detect neutrons by the time-of-flight method.

To meet these requirements and improve the ND280 performance, a near detector upgrade was launched by the T2K collaboration in 2017 [4]. The new detectors, a 3D fine grained fully-active plastic scintillator detector (SuperFGD), two High-Angle TPCs, read out by resistive Micromegas detectors surrounded by six large TOF planes, as shown in Figure 1, were designed and constructed.

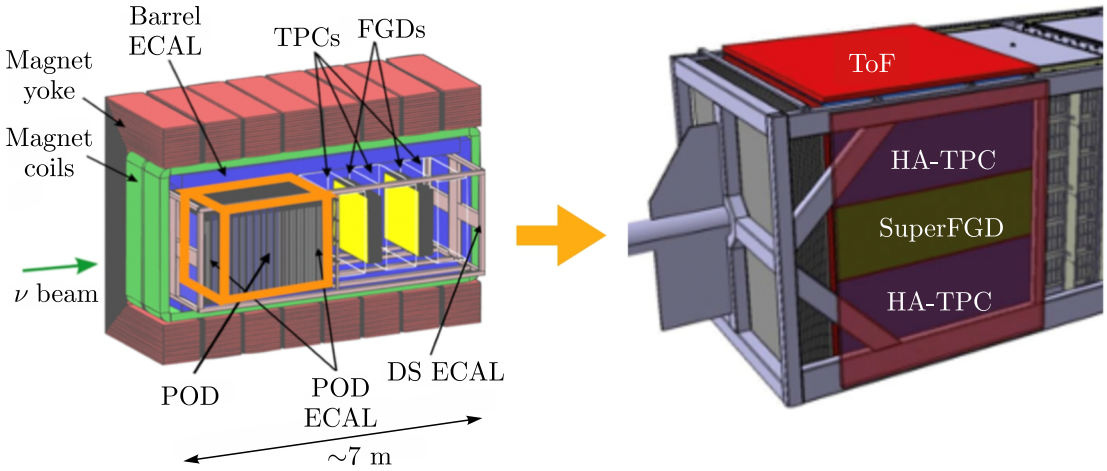

Figure 1. The T2K near detector ND280 before the upgrade (left) and after the upgrade (right).

This paper is based on the talk presented at the session-conference of the Nuclear Physics Section, PSD RAS, dedicated to the 70th anniversary of the birth of V. A. Rubakov.

2. Description of SuperFGD

A schematic view of SuperFGD is shown in Figure 2. SuperFGD consists of about 2×10^6 small scintillation cubes of 1 cm size. The scintillator cubes are produced at the UNIPLAST Co.

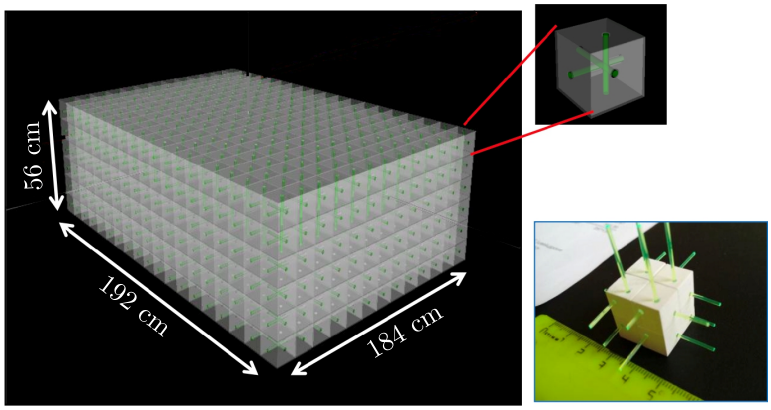

Figure 2. Schematic view of SuperFGD. Also shown are scintillator cubes with wavelength-shifting (WLS) fibres inserted.

(Vladimir, Russia) by injection moulding. The scintillator composition is the optical quality polystyrene doped with 1.5% of paraterphenyl (PTP) and 0.01% of POPOP. After extraction from a press form the cubes were covered with a reflecting layer by etching the scintillator surface with a chemical agent. The etching results in the formation of a white polystyrene micropore deposit of 50–80 μm over the scintillator with good diffuse reflective performance. Three orthogonal through holes of 1.5 mm diameter are drilled in the cubes for WLS fibres. Signals from each cube are read out via three orthogonal 1.0 mm Kuraray Y11 fibres inserted in the holes. One end of each fibre is viewed by the photosensor Hamamatsu MPPC S13360-1325PE.

2.1. SuperFGD assembly procedure

A total of $\sim 2 \times 10^6$ cubes were produced within 2 years. The precision of the size of the cubes was about 30 μm. To check the precision of the holes, small planes of 15×15 cubes with stainless steel knitting needles with a diameter of 1.3 mm inserted into the orthogonal holes were assembled. In the case of a good match of the sizes and the holes of the cubes, all 30 needles had to pass freely through the holes. If the needle has not passed freely through 15 holes in a row, the cube(s) responsible for this kind of misalignment should be removed and replaced with others. In order to check 3rd hole in each cube, cubes in 15 needles are turned by 90 degrees and the procedure with the insertion of the needles is repeated again. This step completes the 3D test of 225 cubes assembled in a 15×15 array. This selection allowed for a precision of the hole position relative to the side of the cube of about 40 μm. Then, a prepared fishing line 2.5 m long and 1.3 mm in diameter inserted into holes of 192 cubes from the tested 15×15 array makes a string of cubes. The 182 strings were aligned in such a way that the horizontal holes of the corresponding cubes in the adjacent strings make a line, so one can insert a 1 m long welding rod of 1.2 mm diameter into this long hole. Finally, 192 such welding rods make a half of the layer with very well aligned 192×92 cubes. Then after fitting of two halves of the plane the rods are extracted one by one, and fishing lines are inserted instead, forming a detector plane. Several detectors planes, each of 192×184 cubes, assembled using fishing lines are shown in Figure 3. All 56 planes assembled with fishing lines were installed in the mechanical box with the holes to let both ends of all the fishing lines to exit it, as shown in Figure 4 (left). Then all fishing lines were replaced by WLS fibres which are coupled, on one side, with the MPPCs and, on the other side, with the LED light guide plate, as can be seen in Figure 4 (right). After the box was fully assembled, a maximum sagging of 3 mm was measured in the center of the bottom panel. The scintillation light is detected by Hamamatsu Multi-Pixel Photon Counters (MPPCs) S13360-1325PE with a sensitive area of 1.3×1.3 mm which are designed to match the 1 mm diameter of the Kuraray double-clad Y11 WLS fibres. The MPPCs were mounted on custom printed circuit boards with a 1 cm pitch in 8×8 arrays

Figure 3. Several SuperFGD planes assembled using fishing lines. Each plane is an array of 192×184 cubes.

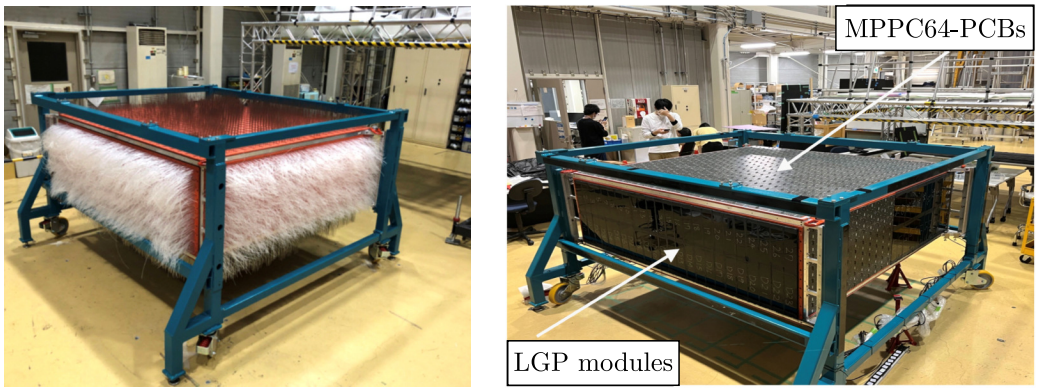

Figure 4. SuperFGD assembled with fishing lines (left); SuperFGD completely assembled in the box with WLS fibers, LGP modules and MPPC64-PCBs (right).

(MPPC64-PCBs). The use of PCBs provides a precise optical alignment and simplifies the detector assembly.

2.2. LED calibration system

The calibration and monitoring of MPPC's gain was provided by an LED calibration system which was installed at the opposite ends of the WLS fibres from the MPPCs. To provide a sufficient light yield of a few photoelectrons in each readout channel, a uniform LED light distribution across many channels is required. In addition, the LED system should be compact due to space constraints. To meet these requirements, a light guide plate (LGP) was adopted as the optical distributor (Figure 5). Based on an LED-based calibration system developed

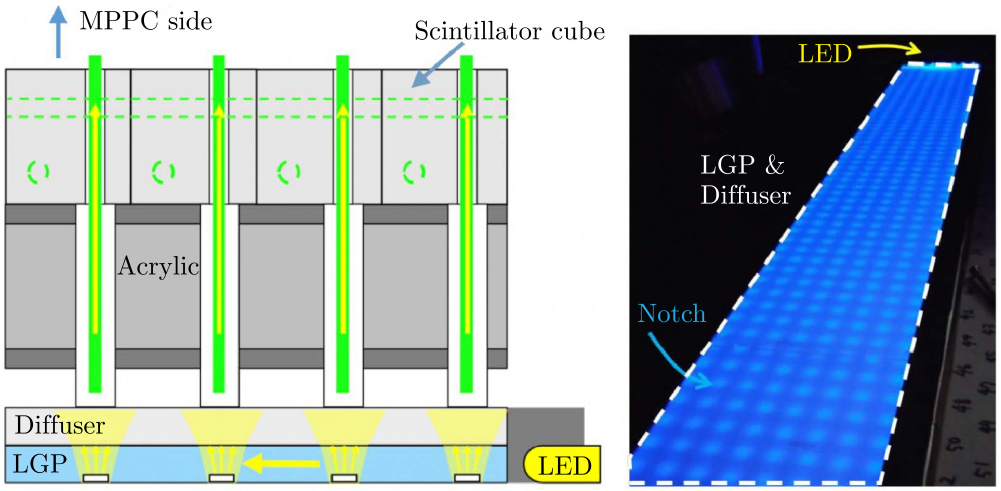

Figure 5. The LED calibration system. The general scheme of the LED system (left), an LGP with notches and diffuser (right).

by the CALICE collaboration [5], the SuperFGD calibration system uses 8 mm thick notched LGPs. The blue LED light which enters the side of the LGP is scattered by the notches aligned with the ends of fibres and absorbed by WLS fibres. Then the re-emitted light is transmitted to MPPCs.

2.3. Readout electronics

The readout of MPPCs is provided by 222 front-end boards (FEBs) organized in 16 crates positioned on the sides of the detector. Each crate includes a backplane for power and signal distribution, and an optical concentrator board (OCB) for transmitting data, trigger, and clock

signals. The FEB equipped with eight CITIROC ASICs [6, 7] and one FPGA amplifies, shapes and digitizes the signals for 32 channels, measures the signal times, and performs slow control operations. CITIROC provides both high-gain and low-gain shaped signals allowing a wide dynamic range. Outside of the CITIROC, two 8-ch 12-bit ADCs digitize the multiplexed high-gain and low-gain output. The CITIROC additionally provides timing information using a constant threshold discriminator on the amplified signal, shaped with a 12.5 ns peaking time shaper. Timing information is extracted using a fast shaper and discriminator with adjustable thresholds. The time over threshold (ToT), defined by the difference between the rising and falling edges of the signal, provides an additional measurement of the signal amplitude. Readout electronics has a wide dynamic range: high gain of 3.5–180 p.e., low gain covers the interval of 150–1500 p.e., and the dead time free ToT measures the light yield up to 1000 p.e.

The data acquisition and slow control systems are based on the MIDAS framework, which is shared with other ND280 subdetectors, facilitating integration and unified operation.

3. Parameters of scintillator cubes

The parameters of the scintillator cubes were measured in the tests with positively and negatively charged particles in the momentum interval from 0.4 to 8 GeV at CERN, using a $5 \times 5 \times 5$ and an $8 \times 24 \times 48$ cube arrays [8, 9]. The $8 \times 24 \times 48$ cube array prototype was tested with a 0.2 T magnetic field, similar to the magnetic field in the ND280 detector. It was obtained that the typical light yield (l.y.) was about 40 p.e./MIP/fibre, and the total l.y. from two fibres in the same cube measured on an event-by-event basis was about 80 p.e., as expected. Muon/pion, and proton hit amplitude samples are clearly distinct for a given momentum. In the case of protons, l.y. varied from 100 up to 450 p.e./fibre at the end of the proton track. An optical crosstalk was measured as a ratio of signals in adjacent cubes to the signal in the fired cube. The average value of the optical crosstalk from cube to cube was found to be 3.7% [10]. The timing of a cube was obtained as the average time between the two readout fibres. The typical time resolution (σ_t) for a single fibre was about 0.95 ns [11]. A cube with two readout fibres gives $\sigma_t = 65-0.71$ ns. Averaging the time from 2 scintillator cubes with 2 fibres each improves the time resolution to 0.47 ns. It seems that a very good time resolution can be achieved for neutrons since recoil protons or other produced particles hit typically several cubes and produce larger amplitudes than muons in each cube.

4. SuperFGD calibration

All scintillator cubes were produced and selected for the detector assembly in 2019–2021. A total of 57 layers, including one spare, each of 184×192 cubes, were assembled using fishing lines at INR and shipped to J-PARC in June 2022. The construction of SuperFGD was completed in April 2023, and on-surface tests and calibration using LED calibration system and cosmics had immediately begun and continued for about 5 months until the detector installation in the ND280 pit in September 2023. The SuperFGD data acquisition software was implemented and tuned during these on-surface tests. A typical vertical muon track is shown in Figure 6. The 3D geometry of SuperFGD allows one to precisely measure the attenuation length of each of 55 888 WLS fibres using cosmic muons. The light yield is measured independently for each cube along a certain WLS fibre. Its position is determined by the other two orthogonal fibres crossing the same cube. Therefore, it is possible to measure the attenuation length for each WLS fibre. This allows potential non-uniformities between the responses of different readout channels to be visualised and possible broken/damaged fibres to be identified.

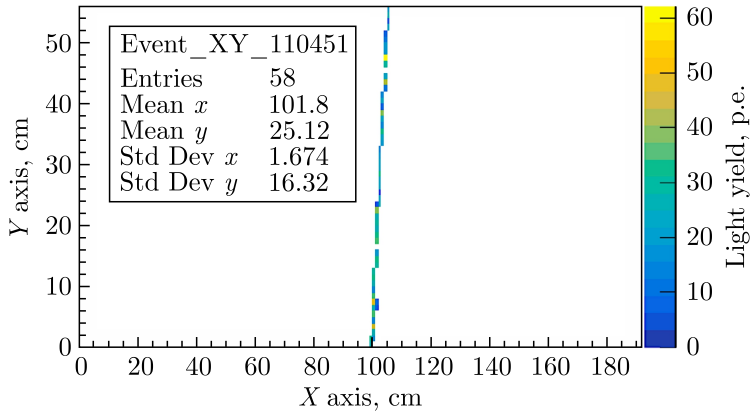

Figure 6. A typical vertical muon track used for the on-surface SuperFGD calibration.

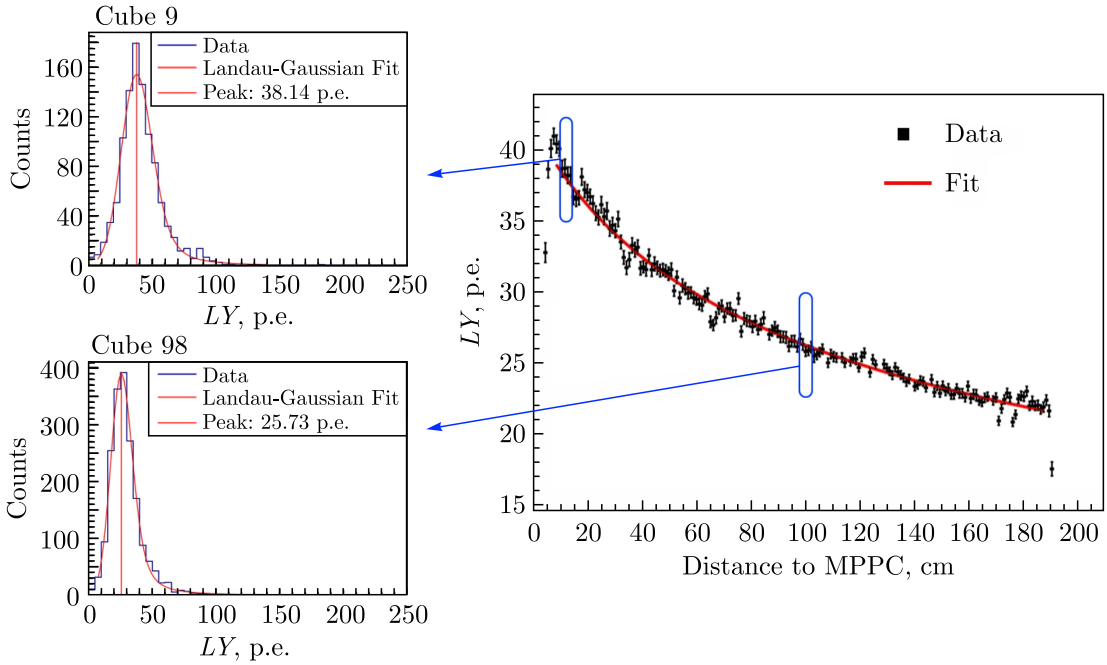

Figure 7. The light yield distribution measured by all the WLS fibres along the Z axis (longitudinal to the main neutrino beam axis) in the bottom layer of cubes. The accumulated events from the first 96 WLS fibres on the left side of the detector are shown for the 9th and 98th cubes along the fibre. The red curve shows the best fit of measured data.

An example of a measured attenuation curve is shown in Figure 7. The attenuation length is measured for each WLS fibre by fitting the light yield as a function of the cube position along the fibre from the MPPC. The light yield $LY(x)$ as a function of the distance x between an MPPC and a cube is parametrized by the following function:

$$LY(x) = LY_0[\alpha e^{-x/A_L} + (1-\alpha)e^{-x/A_S}] + RL_0[\alpha e^{-(2L-x)/A_L} + (1-\alpha)e^{-(2L-x)/A_S}],$$

where LY_0 is the light yield of the first (nearest to MPPC) cube, α is the ratio of the light component of long attenuation length, A_S is the short attenuation length, A_L is the long attenuation length, L is the total length of a fibre. The second term of the expression describes the reflected light from the far end of the WLS fibres with the reflection coefficient R. The best fit of experimental data is obtained using the above expression with the parameters: $LY_0 = 38.6$ p.e., $\alpha = 0.8$, $A_L = 285$ cm, $A_S = 32$ cm, $R = 0.37$.

As was mentioned above, SuperFGD can provide a sub-nanosecond time resolution on the single-cube response. This opens good prospects for detecting neutrons produced by antineu-

trino interactions in SuperFGD and reconstructing their kinetic energy by measuring the time of flight. Since the recoil protons or other produced particles from neutron interactions hit typically several cubes and in addition produce larger amplitudes than muons, the times resolution $\sigma_t \sim 0.2{-}0.3$ ns can be obtained, as follows from the study [11]. SuperFGD has a capability to identify stopped pions and muons by the measurement of time delay with respect to that of the neutrino interaction. The time distribution of particles produced in the decay of cosmic muons (positive and negative) stopped in SuperFGD is shown in Figure 8. The obtained decay

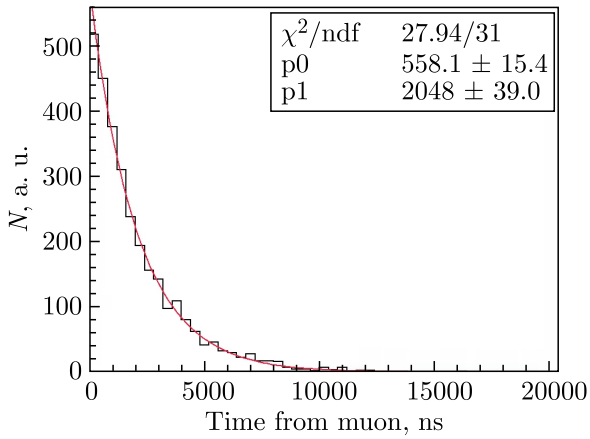

Figure 8. Time distribution of Michel electron events from a sample of stopped cosmic positive and negative muons. The fit with an exponential function shows a decay time of 2.05 μs.

time value of 2.05 μs is slightly lower than 2.2 μs, due to the capture of a fraction of μ^- before the decay.

5. SuperFGD commissioning in the T2K neutrino beam

SuperFGD, top and bottom High-Angle TPCs, and TOF detector were successfully installed into the ND280 magnet in May 2024. The new configuration of ND280 is shown in Figure 9. Figure 10 shows the CCQE event with detection of a muon and a proton in SuperFGD. The

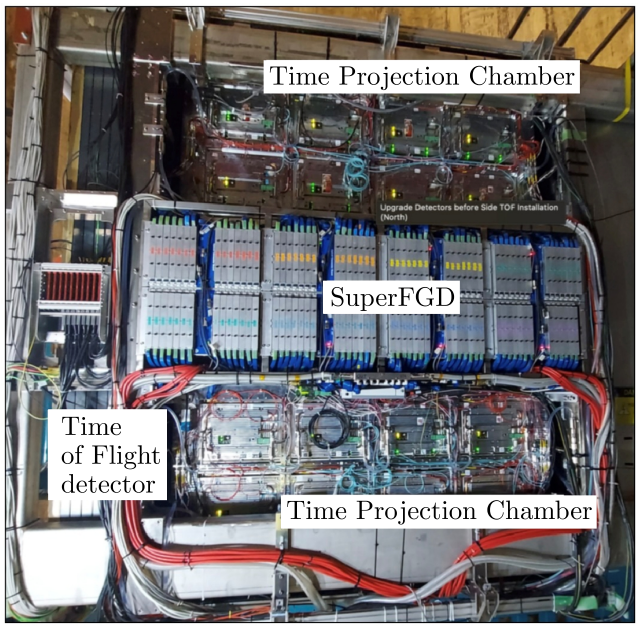

Figure 9. The new ND280 detectors installed in the magnet: SuperFGD, High-Angle TPCs, and TOF.

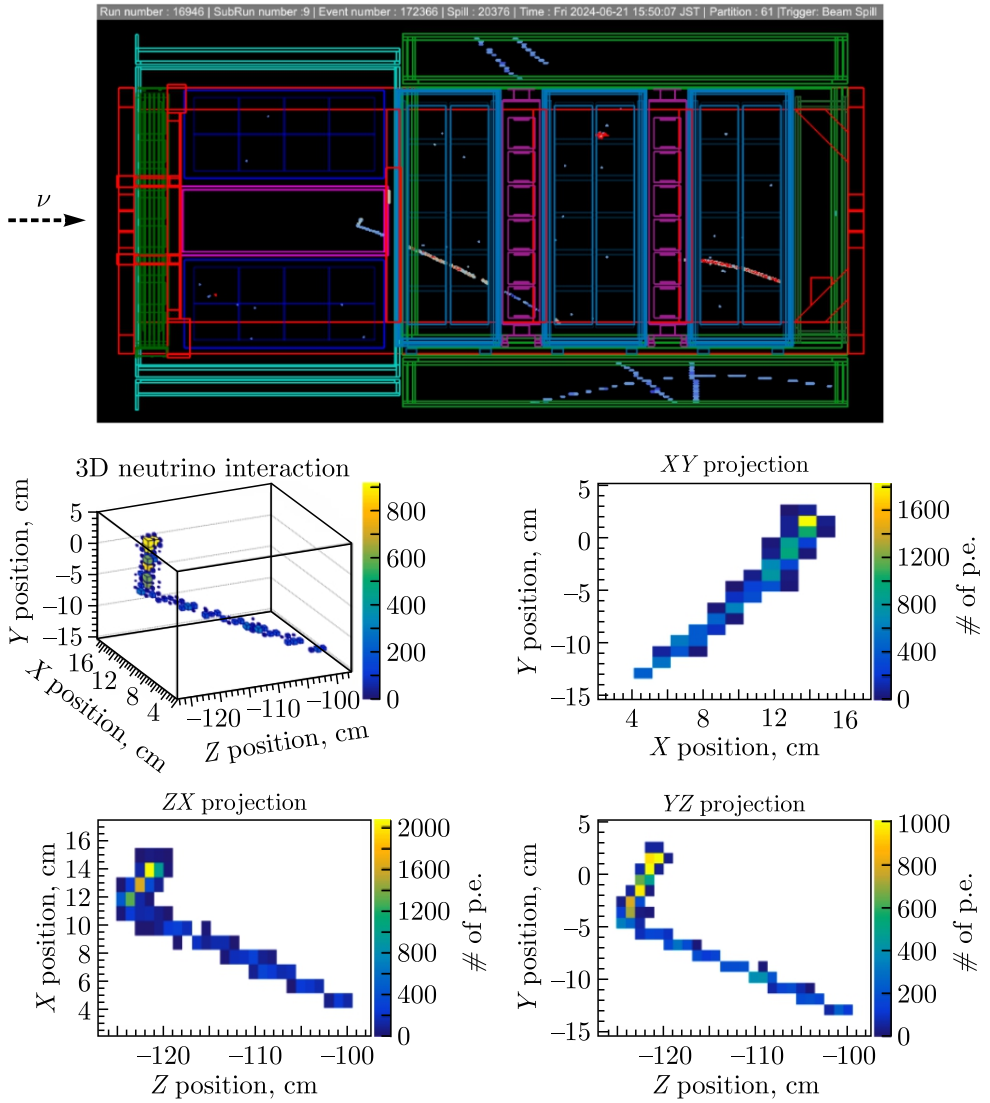

Figure 10. Neutrino charged-current quasi-elastic (CCQE) interaction detected in SuperFGD during the June 2024 run. The final state comprises a muon (long track) also detected in the downstream TPC and one proton stopped in SuperFGD. Top: event display of the whole ND280. Bottom: 3D neutrino interaction reconstructed in X, Y, Z coordinates (top left); 2D views of the event, shown on top right (XY view), bottom left (XZ view) and bottom right (YZ view). The colours in the 3D event show the reconstructed energy loss by the particle in arbitrary units. The size of each voxel is proportional to the energy loss in a specific cube. The colours in the 2D views are in units of p.e., and the size of each bin is just the size of the project cube.

unique feature of SuperFGD to detect short tracks in neutrino interactions is demonstrated in Figure 11. The energy losses of protons which have a short track in SuperFGD are shown in Figure 12.

SuperFGD is the first neutrino detector that can detect high-energy neutrons and reconstruct their energy by measuring the time of flight. Neutron detection occurs by the identification of isolated clusters or tracks that show a Bragg peak feature with a delay of a few nanoseconds with respect to the neutrino interaction. The measurement of the 3D distance and the time difference between the neutrino vertex and the isolated cluster or track allows one to compute the neutron time of flight and, consequently, to define the neutron kinetic energy. An example of the neutron detection in SuperFGD is shown in Figure 13.

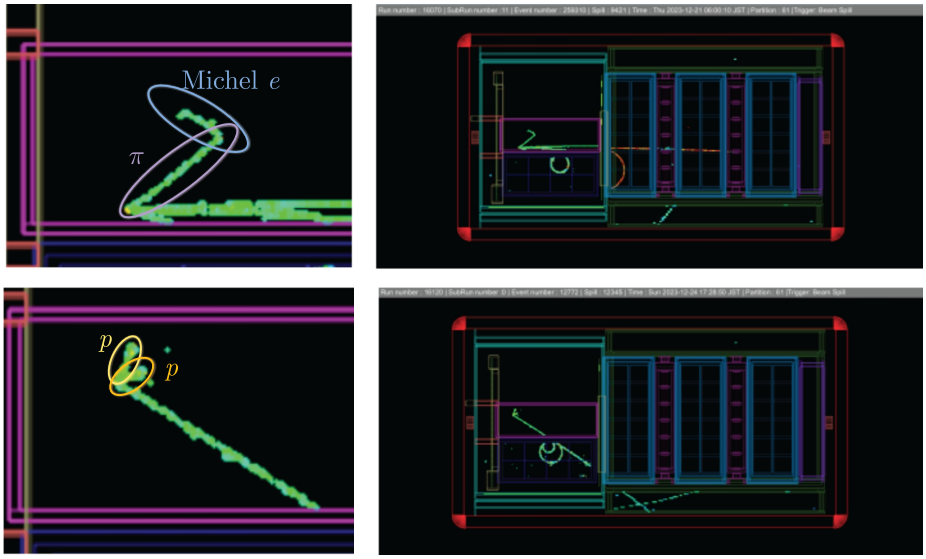

Figure 11. Event display of neutrino events in SuperFGD. Top: charged-current (CC) interaction with a pion in the final state. The Michel electron from the $\pi-\mu-e$ chain is detected in SuperFGD. Bottom: the CC event with a muon and two protons in the final state which have short tracks.

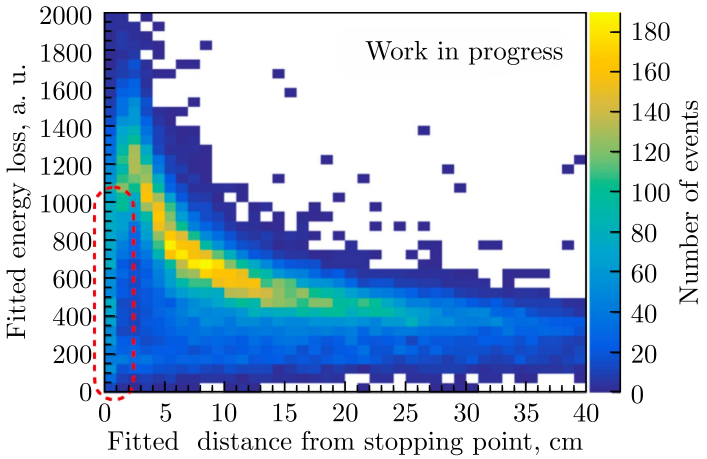

Figure 12. Distribution of the fitted energy loss (in arbitrary units) by protons stopped in SuperFGD. The Bragg peak structure produced by protons is well visible.

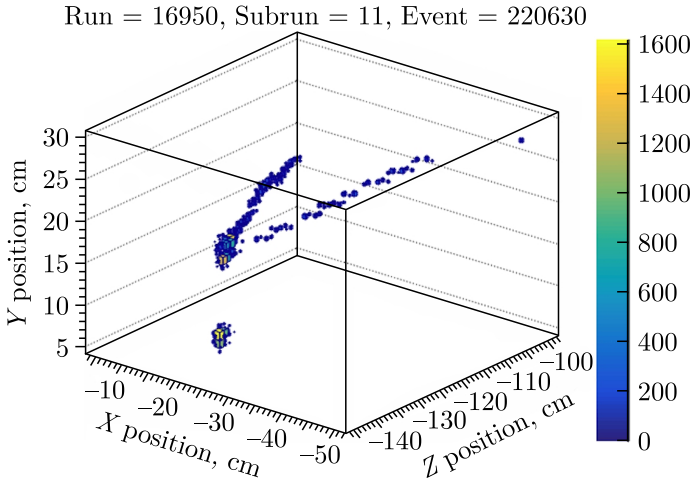

Figure 13. An example of the event of the neutrino charged-current interaction in SuperFGD with a neutron in the final state. The energy losses in each cube are shown in arbitrary units for a 3D reconstructed event.

The neutron kinetic energy can be measured with a resolution between 10–20% for energies up to about 300 MeV [12]. Improving the time resolution will further improve the neutron energy resolution.

6. Conclusion

The SuperFGD consisting of $\sim 2 \times 10^6$ optically isolated scintillator cubes read out by about 56,000 orthogonal WLS fibres and MPPCs will be the central active element of the near neutrino detector complex ND280 of the T2K and HyperKamiokande experiments. The SuperFGD construction was completed in March 2023. Then the detector was installed in ND280 magnet, tested, calibrated with cosmics, and commissioned with T2K neutrinos in October 2023. SuperFGD successfully began collecting neutrino beam data for physics analysis in May 2024.

Due to its unique feature, the SupperFGD provides new opportunities for studying neutrino oscillations. The fine granularity and high scintillation light yield will allow one to accurately track and identify protons stopped in the detector using the Bragg peak down to the momentum of about 300 MeV/c. The pions can also be characterised by the detection of delayed Michel electrons. The 3D granularity and a single-cube time resolution of 0.7 ns for a minimum ionizing particle will ensure an efficient detection and measurement of the neutron energy by time of flight.

Acknowledgements

It is a great pleasure to express my appreciation to all colleagues involved in the design, tests, construction, and commissioning of SuperFGD for their hard work and efforts that have made it possible to successfully build this novel neutrino detector and begin data taking with the T2K neutrino beam.

Author contributions

Author: SuperFGD design, tests, construction, original draft preparation, writing, and editing.

Funding

This work was supported by the Russian Science Foundation grant No. 24-12-00271.

Conflicts of Interest

The author declares no conflicts of interest.

References

[1] K. Abe et al., The T2K experiment, Nuclear Instruments and Methods in Physics Research Section A 659 (2011) 106–135. arXiv:1106.1238, doi:10.1016/j.nima.2011.06.067.

[2] Y. Kudenko, The Near neutrino detector for the T2K experiment, Nuclear Instruments and Methods in Physics Research Section A 598 (2009) 289–295. arXiv:0805.0411, doi:10.1016/j.nima.2008.08.029.

[3] K. Abe et al., Hyper-Kamiokande Design Report. arXiv:1805.04163.

[4] K. Abe et al., T2K ND280 Upgrade — Technical Design Report. arXiv:1901.03750.

[5] J. Kvasnicka and I. Polak, LED calibration systems for CALICE hadron calorimeter, Physics Procedia 37 (2012) 402–409. doi:10.1016/j.phpro.2012.02.379.

[6] D. Impiombato et al., Characterization and performance of the ASIC (CITIROC) front-end of the ASTRI camera, Nuclear Instruments and Methods in Physics Research Section A 794 (2015) 185–192. arXiv:1506.00264, doi:10.1016/j.nima.2015.05.028.

[7] O. Basille et al., Baby MIND readout electronics architecture for accelerator neutrino particle physics detectors employing silicon photomultipliers, JPS Conference Proceedings 27 (2019) 011011. doi:10.7566/JPSCP.27.011011.

[8] O. Mineev et al., Beam test results of 3D fine-grained scintillator detector prototype for a T2K ND280 neutrino active target, Nuclear Instruments and Methods in Physics Research Section A 923 (2019) 134–138. arXiv:1808.08829, doi:10.1016/j.nima.2019.01.080.

[9] A. Blondel et al., The SuperFGD prototype charged particle beam tests, Journal of Instrumentation 15 (12) (2020) P12003. arXiv:2008.08861, doi:10.1088/1748-0221/15/12/P12003.

[10] A. Artikov et al., Investigation of light collection in scintillation cubes of the SFGD detector, Physics of Particles and Nuclei Letters 19 (2022) 784–791. doi:10.1134/S1547477122060036.

[11] I. Alekseev et al., SuperFGD prototype time resolution studies, Journal of Instrumentation 18 (01) (2023) P01012. arXiv:2206.10507, doi:10.1088/1748-0221/18/01/P01012.

[12] L. Munteanu, S. Suvorov, S. Dolan, D. Sgalaberna, S. Bolognesi, S. Manly, G. Yang, C. Giganti, K. Iwamoto, and C. Jesús-Valls, New method for an improved antineutrino energy reconstruction with charged-current interactions in next-generation detectors, Physical Review D 101 (9) (2020) 092003. arXiv:1912.01511, doi:10.1103/PhysRevD.101.092003.